A unified model for ULXs and ULSs;

Radiation hydrodynamic simulations of super-Eddington accretion flows

Takumi Ogawa (Kyoto University),
Shin Mineshige (Kyoto University),
Tomohisa Kawashima, Ken Ohsuga (NAOJ)

Ultra-Luminous Supersoft sources (ULSs)
vs
Ultra-Luminous X-ray sources (ULXs)

	ULXs	ULSs
Luminosity	$> 10^{39}\ \mathrm{erg\ s^{-1}}$	$\gtrsim 10^{39}\ \mathrm{erg\ s^{-1}}$
Typical temperature	$\gtrsim 1\ \mathrm{keV}$	$\lesssim 0.1\ \mathrm{keV}$

similar

different

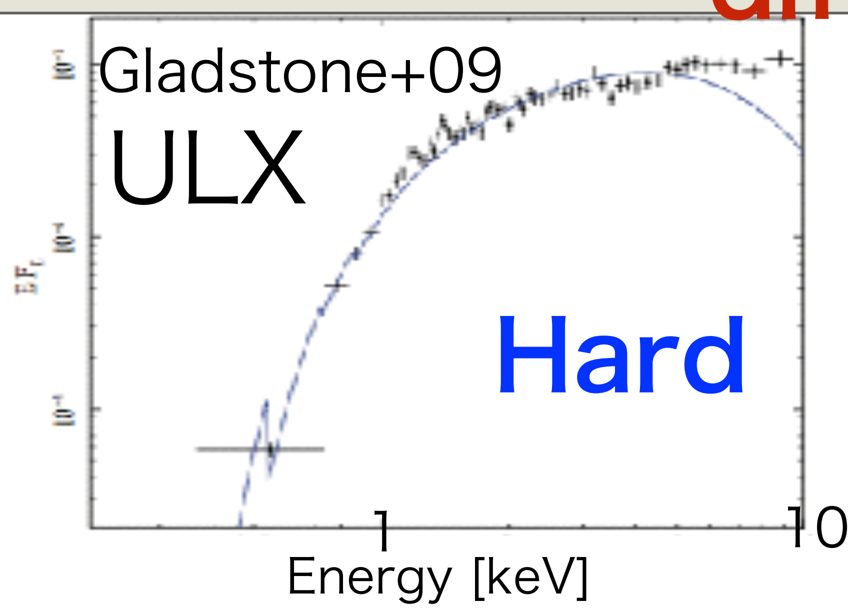

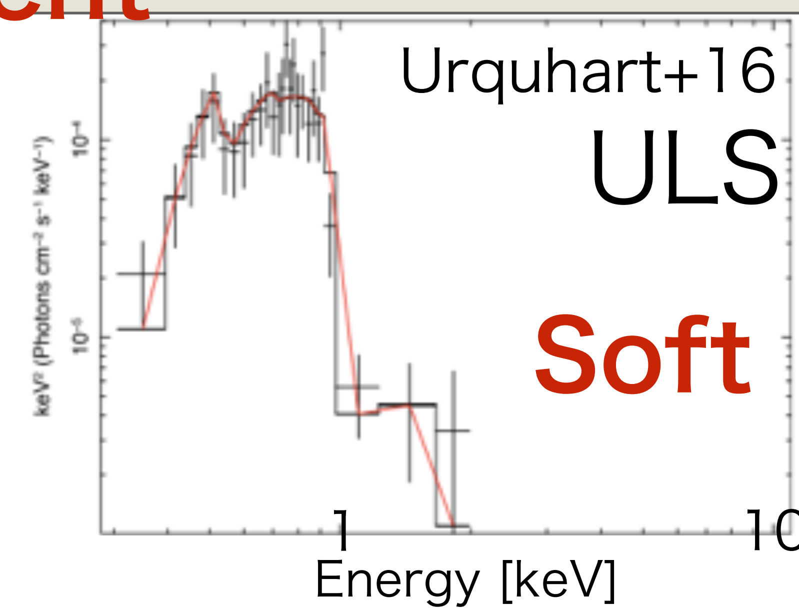

Are ULSs also **super-Eddington accretors** onto stellar mass compact objects ?

If so,

What produces the difference between ULSs and ULXs?

Unified Model for these Ultra-Luminous sources

Both ULXs and ULSs are super-Eddington accretors

But

difference is mainly generated by the viewing angle

(Urquhart & Soria 2016)

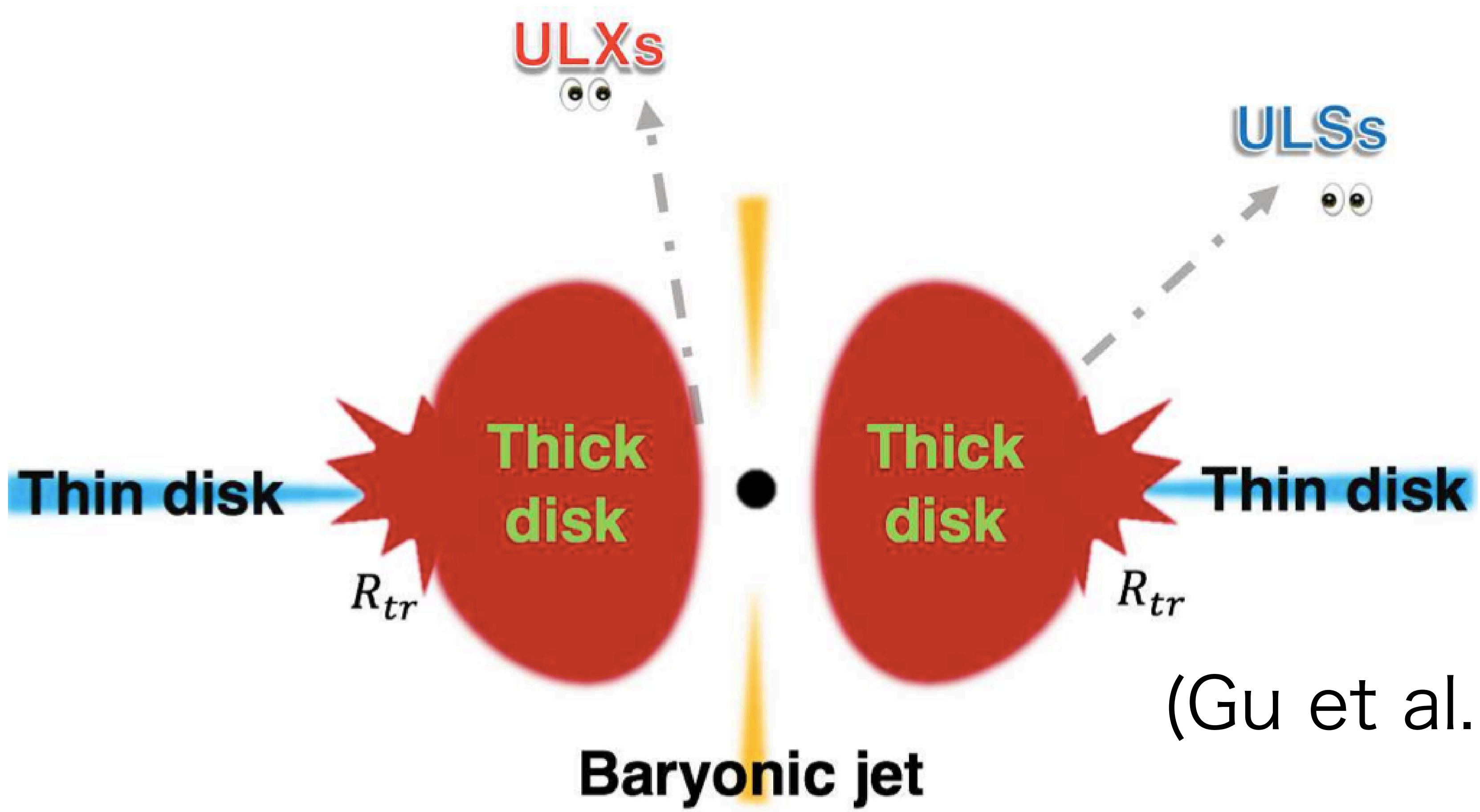

(Gu et al. 2015)

when viewing from the polar direction → **ULXs**

when viewing from the horizontal direction → **ULSs**

Motivation and Goals

Key Questions

- How are super-Eddington accretion flows observed and how does their appearance vary, depending on the viewing angle?

- **Can the basic properties of ULSs be explained by the super-Eddington scenario?**

In the present study,
we performed 2D axisymmetric radiation hydrodynamic simulations of super-Eddington accretion flows for various accretion rates

Basic Equations

Radiation Hydrodynamics with the Flux Limited Diffusion Approximation

$$\frac{\partial \rho}{\partial t} + \nabla \cdot (\rho \boldsymbol{v}) = 0$$

(mass conservation)

$$\frac{\partial(\rho v_r)}{\partial t} + \nabla \cdot (\rho v_r \boldsymbol{v}) = -\frac{\partial p}{\partial r} + \rho \left[\frac{v_\theta^2}{r} + \frac{v_\varphi^2}{r} - \frac{GM_{\rm BH}}{(r - r_{\rm S})^2} \right] + f_r + q_r$$

$$\frac{\partial(\rho r v_\theta)}{\partial t} + \nabla \cdot (\rho r v_\theta \boldsymbol{v}) = -\frac{\partial p}{\partial \theta} + \rho v_\varphi^2 \cot\theta + r f_\theta + r q_\theta$$

(equation of motion)

$$\frac{\partial(\rho r \sin\theta \, v_\varphi)}{\partial t} + \nabla \cdot (\rho r \sin\theta \, v_\varphi \boldsymbol{v}) = r \sin\theta \, q_\varphi$$

$$\frac{\partial e}{\partial t} + \nabla \cdot (e \boldsymbol{v}) = -p \nabla \cdot \boldsymbol{v} - 4\pi\kappa B + c\kappa E_0 + \Phi_{\rm vis} - \Gamma_{\rm Comp}$$

(energy conservation)

$$\frac{\partial E_0}{\partial t} + \nabla \cdot (E_0 \boldsymbol{v}) = -\nabla \cdot \boldsymbol{F_0} + \nabla \boldsymbol{v} : \boldsymbol{P_0} + 4\pi\kappa B - c\kappa E_0 + \Gamma_{\rm Comp}$$

$$p = (\gamma - 1) e$$

(equation of state)

$$\Gamma_{\rm Comp} = 4 c \sigma_{\rm T} \frac{k_{\rm B}(T_{\rm gas} - T_{\rm rad})}{m_e c^2} \left(\frac{\rho}{m_p} \right) E_0$$

including Thermal Compton effect

Method

- 2D axisymmetric radiation hydrodynamic code (Kawashima+09) with sufficiently large simulation domain($r \in [2r_S, 5000r_S]$ for high$\dot{M}_{\rm inj}$)
- We inject mass at a constant rate $\dot{M}_{\rm inj}$ and with a constant angular momentum from the edge of the disk.
- We calculate 3 cases of different $\dot{M}_{\rm inj}$

$$\dot{M}_{\rm inj}/\dot{M}_{\rm Edd} = 10^2, 10^3, 10^4$$

$$\dot{M}_{\rm Edd} = L_{\rm Edd}/c^2$$

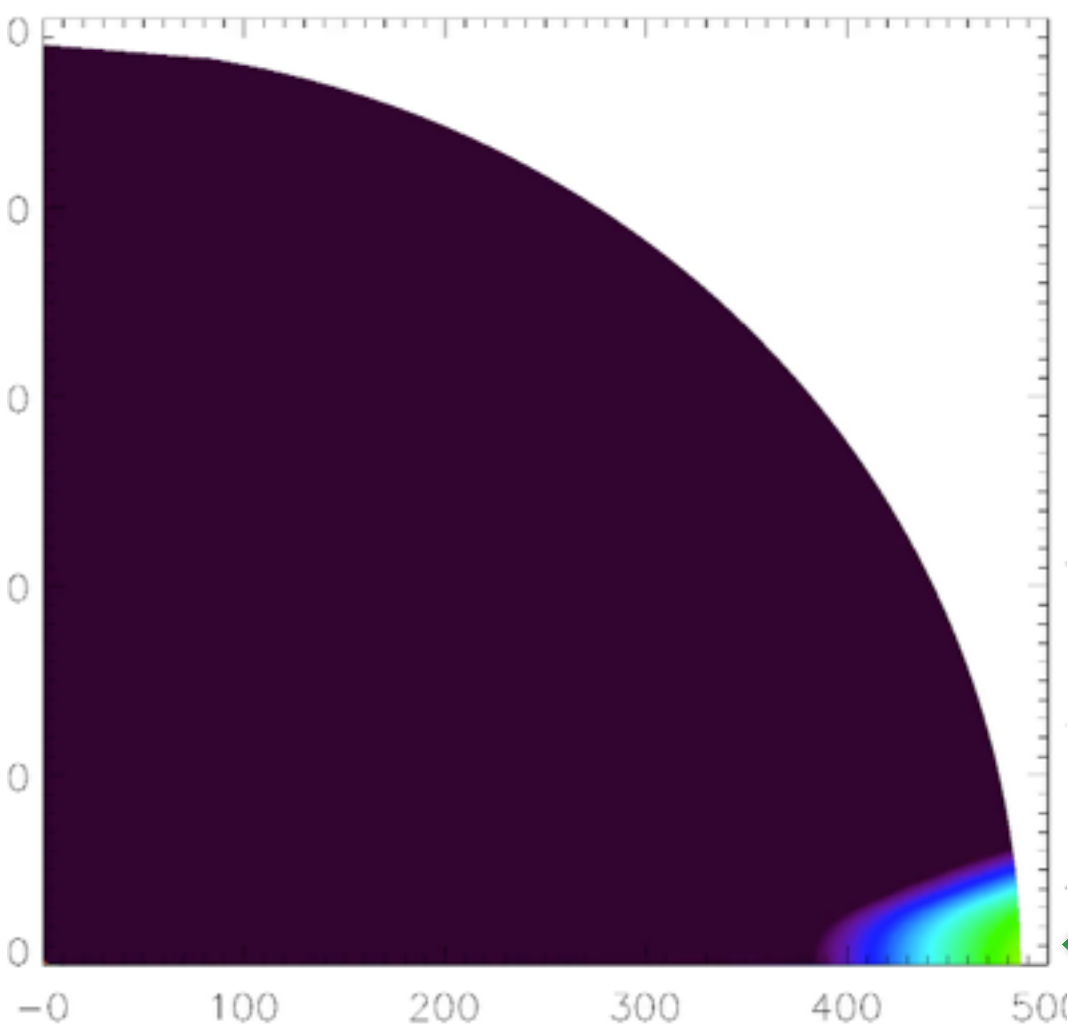

mass injection $\dot{M}_{\rm inj}$

Simulation Overviews

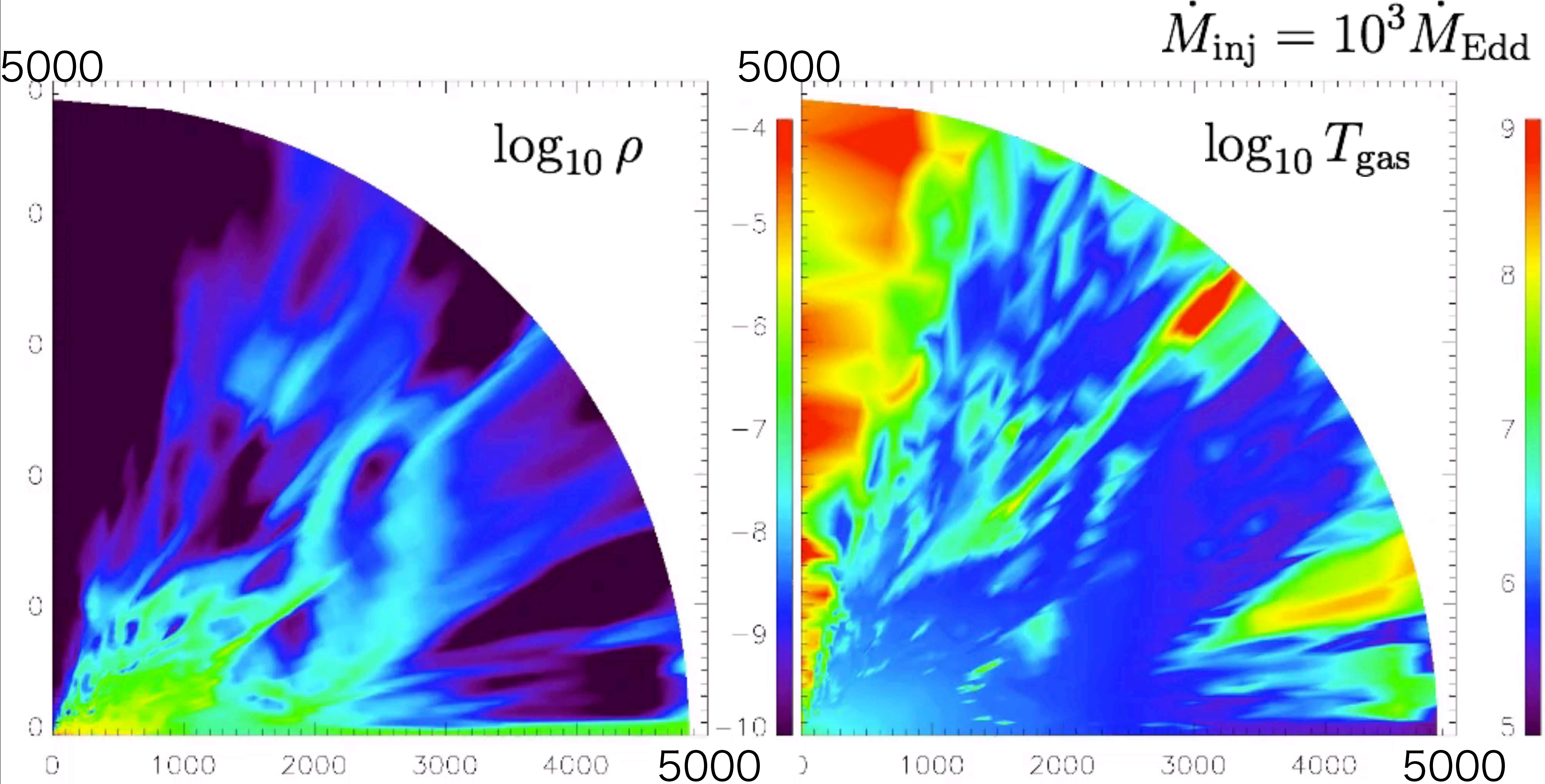

Simulation Overviews

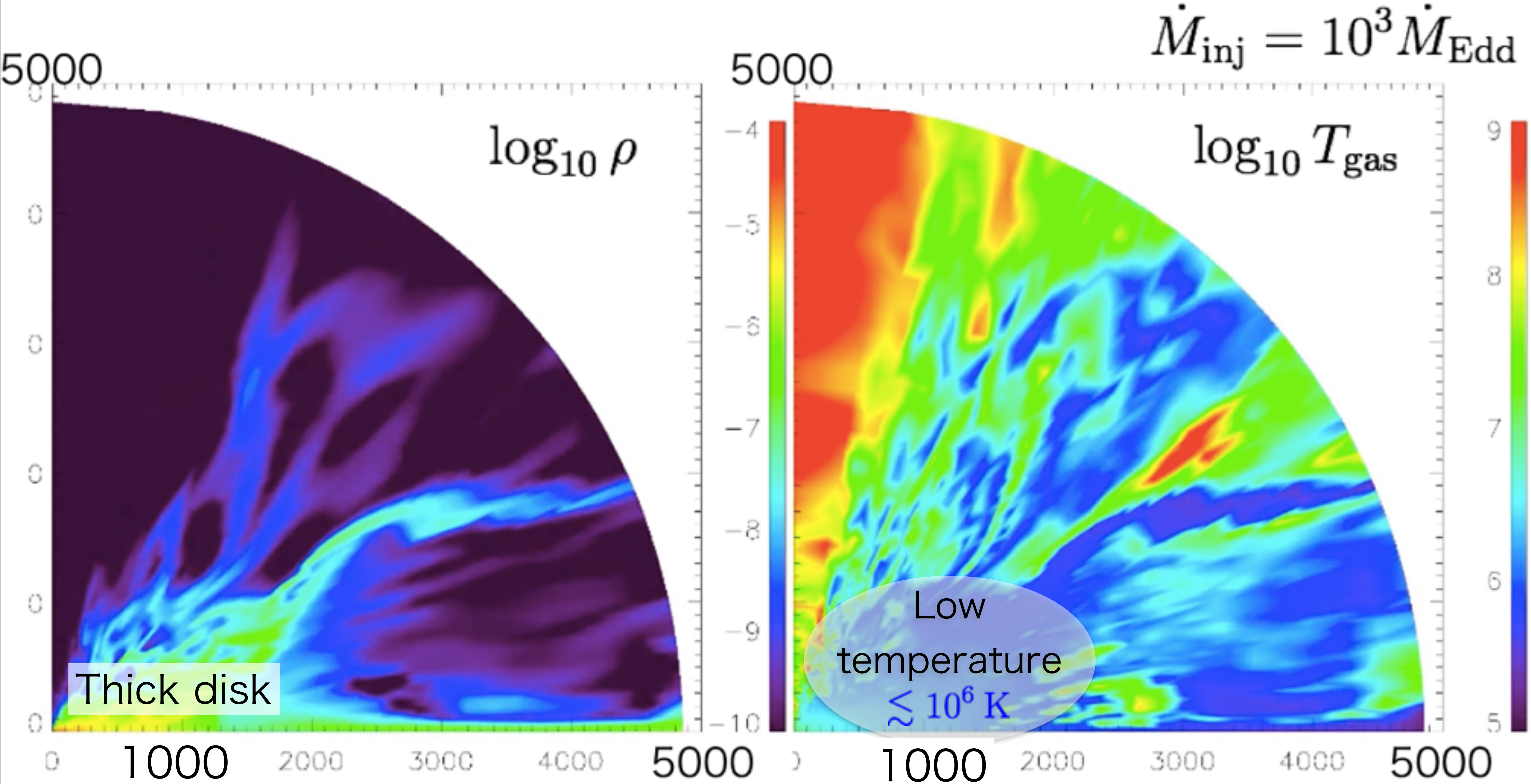

Near the thick disk,
gas temperature goes down to 0.1 keV or smaller.

temperature structure

Time-averaged contour maps of gas temperature

$$T = \langle \rho T_{\rm gas} \rangle / \langle \rho \rangle$$

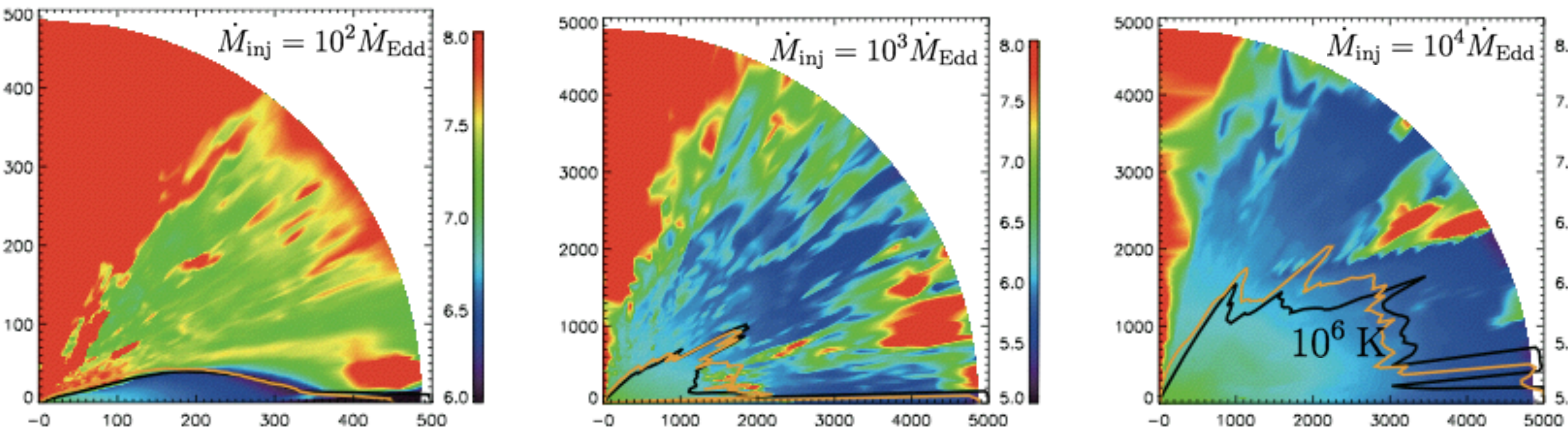

Yellow line: Compton sphere,

$$y_{\rm Comp} \equiv \tau_{\rm es} \int_r^{r_{\rm out}} \frac{4kT}{m_e c^2} \kappa_{\rm es} \rho \, dr = 1$$

Black line: Photosphere

$$\tau_{\rm eff} \equiv \int_r^{r_{\rm out}} \kappa_{\rm eff} \rho \, dr = 1$$

Low $\dot{M}_{\rm acc}$ High

High $T_{\rm gas}$ Low

Observed Temperature and Luminosity

$T(\theta)$:the temperature on the outer sphere between Compton- and photo- spheres

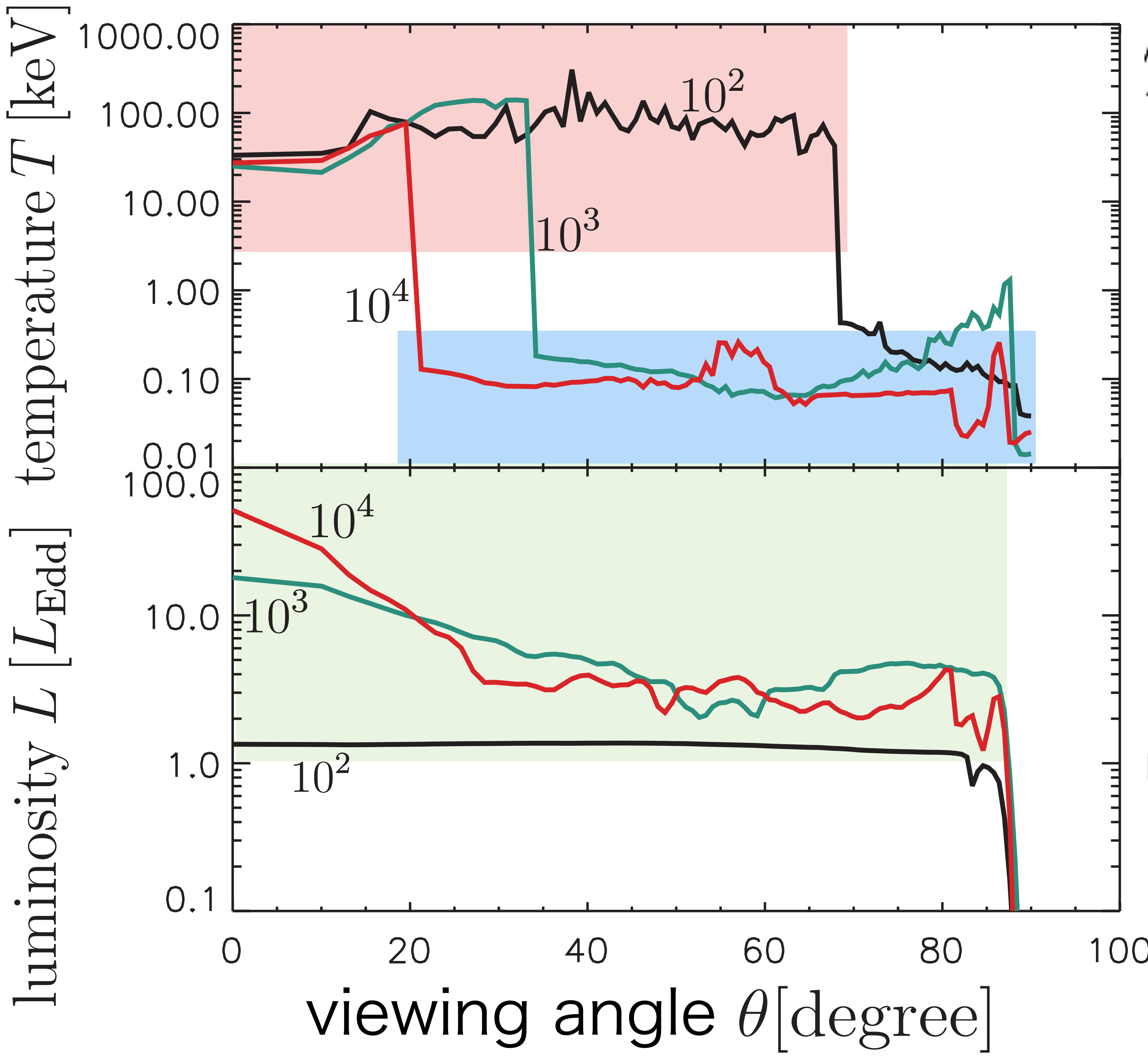

$T \gtrsim$ few keV ⇒ **ULX**

$T \lesssim 0.1$ keV ⇒ **ULS**

$\theta \gtrsim 68^\circ$ for $M_{\rm inj} = 10^2$

$\theta \gtrsim 34^\circ$ for $M_{\rm inj} = 10^3$

$\theta \gtrsim 21^\circ$ for $M_{\rm inj} = 10^4$

⇒ Super-Eddington

ULSs are also super-Eddington accretors

but viewed from large polar angles.

Classification of ULXs and ULSs

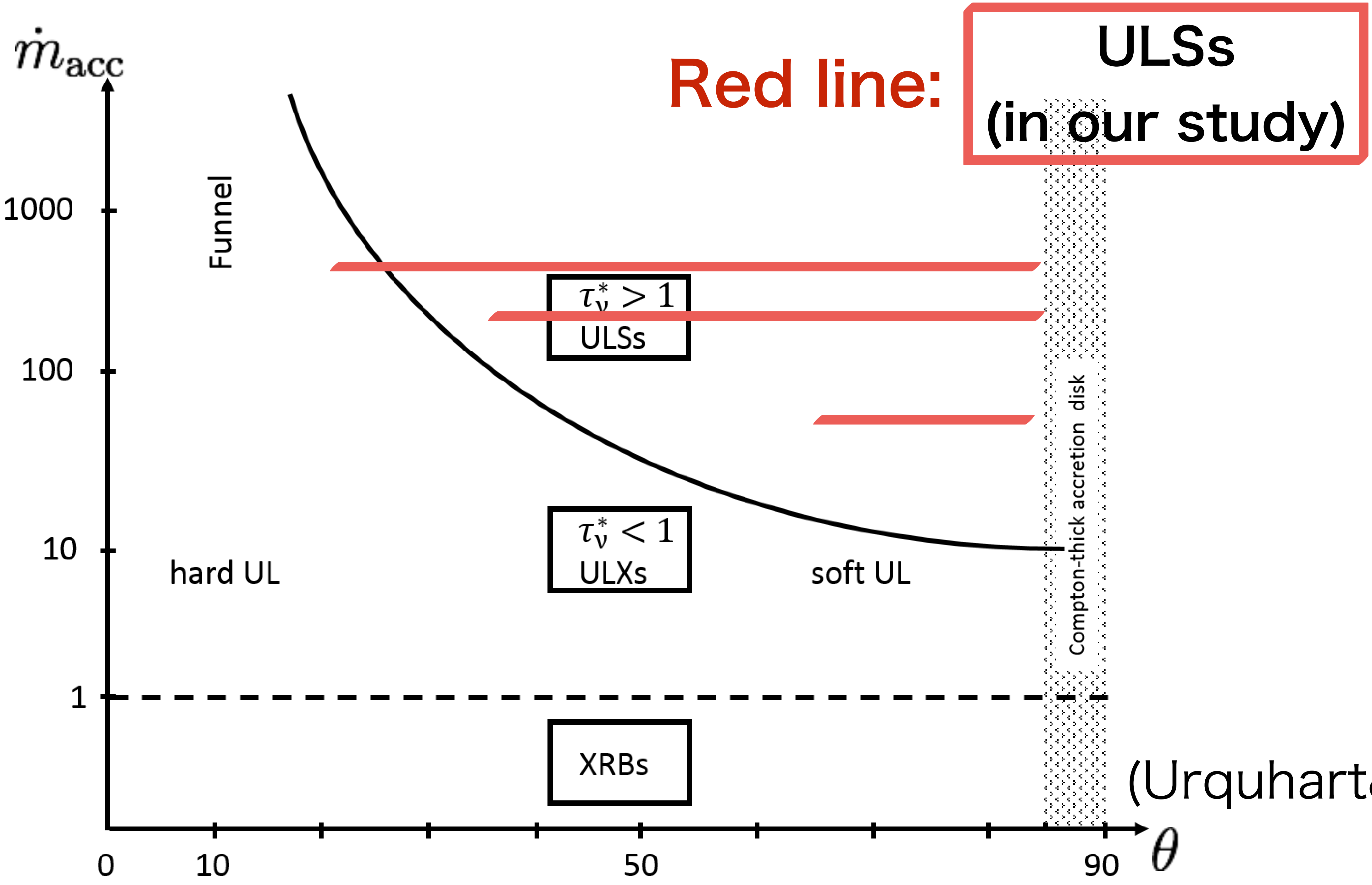

(Urquhart&Soria 2016)

When the accretion rate is larger,

the source is more likely to be seen as ULSs

Summary

Our 2D RHD simulations show

- Both ULXs and ULSs can be super-Eddington accretors,
- The main differences between ULSs and ULXs are

  viewing angle

- The higher mass accretion rate is, the more likely to be observed as a ULS the source is.

Our result supports the Unified model for ULXs and ULSs

In this study, we simply use the temperature on the Compton- or photo- spheres and its luminosity to determine whether an Ultra-Luminous source is a ULS or not.

→ Spectral calculation is needed at a next step